Comparative Study of the Catalytic Amination of Benzylic C-H Bonds Promoted by Ru(TPP)$(py)_2$ *vs.* Ru(TPP)(CO).

Gabriele Manca,[a]* Carlo Mealli,[a] Daniela Maria Carminati,[b] Daniela Intrieri[b] and Emma Gallo[b]*

Abstract: A combined experimental and DFT-based theoretical analysis describes the influence of the axial ligand (L) on the catalytic activity of Ru(porphyrin)L complexes to promote the amination of C-H bonds by organic azides (RN_3). Experimental data indicate that the catalytic activity of Ru(TPP)$(py)_2$ (**2**) (TPP = dianion of tetraphenylporphyrin and py = pyridine) is comparable to that of already studied Ru(TPP)(CO) (**1**). DFT studies disclose a possible mechanism for the C-H bond amination reaction promoted by [Ru]$(py)_2$ (**2'**) ([Ru] = Ru(porphine)). Upon the endergonic departure of one pyridine ligand from **2'**, the unsaturated species [Ru](py) (**11'**) promotes the eco-friendly dismissal of N_2 from RN_3 generating the *mono*-imido complex [Ru](NR)(py) (**6'**) which can access two different spin states of relatively close energy. In the triplet $[Ru](NR)(py)_T$, the diradical character of the imino N atom is responsible for the homolytic activation of the benzylic C-H bond of toluene and then, thanks to a '*rebound mechanism*', the benzylic amine $PhCH_2N(R)H$ is formed. Alternatively, over the singlet PES the remaining pyridine ligand can depart from [Ru](NR)(py) (**6'**) and, through a second RN_3 activation, the *bis*-imido compound $[Ru](NR)_2$ is obtained as an excellent amination catalyst.

Introduction

New catalytic strategies for the synthesis of nitrogen-containing compounds are important given their usage as precursors in biological and pharmaceutical processes.[1-2]

In order to respond to common requests for a sustainable chemistry, the employment of organic azide (RN_3) as nitrogen sources for the synthesis of aza-compounds[3-10] is constantly growing. In fact, this class of aminating reagents shows a high eco-compatibility and atom efficiency due to the formation of the benign molecular nitrogen as the only by-product of the nitrene ('RN') transfer reaction to an organic molecule. Among all available organic azides, aryl azides are very interesting nitrogen sources because of their convenient reactivity/stability relationship and their easy syntheses from corresponding amines. A more extensive usage of these aminating agents is also favoured by their commercial availability, thanks to an efficient and safe procedure, recently developed by Sigma-Aldrich, to obtain aryl azides in bulk amounts.[11]

[a] Dr. G. Manca, Dr. C. Mealli
Istituto di Chimica dei Composti OrganoMetallici, ICCOM-CNR,
Via Madonna del Piano 10, I-50019 Sesto Fiorentino
E-mail: gabriele.manca@iccom.cnr.it

[b] Dr. D.M. Carminati, Dr. D. Intrieri, Prof. E. Gallo
Department of Chemistry, University of Milan
Via Golgi 19, I-20133 Milan (Italy) and
E-mail: emma.gallo@unimi.it

Supporting information for this article is given via a link at the end of the document.

Metal porphyrin complexes efficiently promote amination reactions of saturated and unsaturated hydrocarbons by aryl azides[12-29] and, in particular, they show very good activity in the amination of activated sp^3 C-H bonds. Ruthenium(II) porphyrins[19,21] are competent catalysts in the synthesis of allylic and benzylic amines and they are also active in the amination of benzylic C−H bonds placed in α or β positions to an ester group yielding biological relevant α- and β-amino esters.[23, 30-32]

One of the most extensively used amination catalyst is the five-coordinated complex Ru(TPP)(CO) (**1**) (TPP= dianion of tetraphenylporphyrin) which bears the π-acceptor CO ligand on the axial position and a vacant coordination site to trigger a catalytic reactivity by the azide activation. Considering that catalytic reactions are not necessarily hindered by the presence of a sixth ligand on the metal centre,[33] here we would like to compare the catalytic activity of Ru(TPP)CO (**1**) with that of Ru(TPP)$(py)_2$ (**2**), where two pyridine ligands, with essentially no π-acceptor character and reduced σ-donor features, are present on axial positions. Even though the chemico-physical properties of **2** have been elucidated by a variety of experimental methods such as electrochemistry,[34-35] UV-vis absorption, emission, resonance Raman[36-40] and picosecond transient absorption,[41-42] the use of this complex as a catalyst of the C-H bond amination by organic azides has not yet been reported.

The present study combines experimental and theoretical approaches to interpret the catalytic activity of **2** also in the light of our previously reported mechanistic study[27] of the catalytic allylic amination of cyclohexene by ArN_3 promoted by complex **1**. A kinetic study indicated that the reaction of Ru(TPP)CO with ArN_3 first affords the ruthenium *mono*-imido complex Ru(TPP)(NAr)(CO) which has never been experimentally observed. The theoretical study disclosed that for a general aryl/alkyl R group the catalytic intermediate Ru(TPP)(NR)(CO) is somewhat more stable in the triplet than in the singlet ground state. Thus a diradical species may be accessed, with two unpaired electrons more localised at the nitrogen atom of the 'RN' imido ligand rather than at the metal itself. This electronic situation allows the radical activation of the cyclohexene substrate which evolves into the desired allylic amine product through a '*rebound mechanism*'.[43] It was also established that, when the *mono*-imido ruthenium complex Ru(TPP)(NR)(CO) remains in the singlet form, the axial CO ligand may be dismissed and the activation of another aryl azide molecule at vacant coordination site yields the *bis*-imido ruthenium complex $Ru(TPP)(NR)_2$. This new species was isolated, characterised[18,20] and demonstrated to be a very active catalyst in the amination of hydrocarbon substrates including cyclohexene.[18, 20] DFT studies revealed that a singlet/triplet interconversion, similar to that described for Ru(TPP)(NR)(CO), is responsible for the formation of the triplet state of $Ru(TPP)(NR)_2$ which activates cyclohexene forming the desired

allylic amine through the '*rebound mechanism*' based on two consecutive couplings of radical species.

In this paper, we want to analyse the role of axial ligands on the ruthenium centre to trigger the catalytic activity of the ruthenium porphyrin complexes. In particular, the major differences between the catalytic activity of the two catalysts bearing a π-acceptor (CO in complex **1**) or a σ-donor (pyridine in complex **2**) axial ligand respectively will be highlighted from an electronic and energetic viewpoint.

Results and Discussion

Experimental studies of the catalytic activity of Ru(TPP)(py)$_2$ (2).

The complex Ru(TPP)(py)$_2$ (**2**), was prepared in accordance to a reported synthetic procedure[40] and used as the catalyst for the reaction between aryl azide (ArN_3) and hydrocarbon substrates to yield aminated compounds **3a**-**3i** reported in Table 1. Except for the synthesis of compound **3c**, 3,5-*bis*(trifluoromethyl)phenyl azide was always employed as the aminating agent.

Data reported in Table 1 indicated that complex **2** is a competent catalyst of C-H bond aminations and its catalytic efficiency is comparable to that of Ru(TPP)CO (**1**) when used as the catalysts for the synthesis of the same compounds.[19, 32] Similar to that observed in **1**-catalysed reactions, Ru(TPP)(py)$_2$ (**2**) was more effective in activating electron deficient azides and in fact the reaction of 4-*tert*-butyl azide with ethylbenzene yielded **3c** only in a low yield (entry 2, Table 1). For all the described reactions, NMR and GC-MS analyses of the crude revealed the formation of ArN=NAr and $ArNH_2$ side products which derive from a partial decomposition of the employed azide.

Considering that in previous reactions catalysed by Ru(TPP)CO (**1**)[19, 32] slightly different experimental conditions were used, the synthesis of compound **3f** was repeated in the presence of complex **1** by using the experimental conditions described in Table 1 giving 90% of the benzylic amine in 1 hour. Even if the yield was better than that registered in the presence of catalyst **2** (entry 5, Table 1), the reaction time increased from 20 minutes to one hour. An attempt was made to enhance the selectivity of the benzylic amine **3f** by reducing the formation of side products. The azide was slowly added to the reaction mixture by a syringe pump over 1.5 hours but unfortunately the reaction yield did not improve. Conversely, the reaction yield was enhanced to 72% by reducing the reaction temperature to 70 °C in parallel the time required to completely convert the azide into **3f** became too long (7.0 h). Clearly, the lower working temperature depressed the formation of side products as well as the activation of the azide which was more effective at the refluxing temperature of cumene (~150 °C).

Considering the biological relevance of *β*-aminoesters, the synthesis of 3-(3,5-*bis*(trifluoromethyl)phenylamino)-3-phenyl-propanoate (**3h**) was studied in more detail by using different experimental conditions. As reported in entry 7 of Table 1, the best yield of the desired **3h** compound (82%) was obtained by using a catalytic ratio **2**/3,5 *bis*(trifluoromethyl)phenyl azide = 1:15 in methyl hydrocinnamate as the reaction solvent.

Table 1. Synthesis of compounds **3a-3i** catalysed by Ru(TPP)(py)$_2$ (**2**).[a]

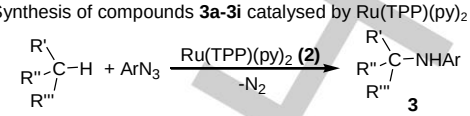

entry	Product	Ar	t (h)[b]	3	yield[c]
1	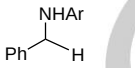	3,5$(CF_3)_2C_6H_2$	0.5	**3a**	62%
2	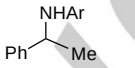	3,5$(CF_3)_2C_6H_2$ 4-^{t}BuC_6H_3	0.6 0.5	**3b** **3c**	85% 32%
3	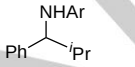	3,5$(CF_3)_2C_6H_2$	0.5	**3d**	50%
4[d]	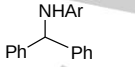	3,5$(CF_3)_2C_6H_2$	0.30	**3e**	65%
5	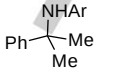	3,5$(CF_3)_2C_6H_2$	0.25	**3f**	61%
6[e]	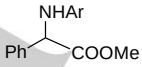	3,5$(CF_3)_2C_6H_2$	12	**3g**	56%
7[e]	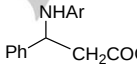	3,5$(CF_3)_2C_6H_2$	8 1.3	**3h**	55% 82%[f]
8	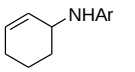	3,5$(CF_3)_2C_6H_2$	0.75	**3i**	77%

[a]Experimental conditions: 6.8×10^{-3} mmol of the catalyst (2% with respect to ArN_3) in 15.0 mL of refluxing hydrocarbon. [b]Time required for the complete azide conversion monitored by IR spectroscopy following the N_3 absorbance decrease at ~2115 cm^{-1}. [c]Yields based on ArN_3 and determined by ^{1}H-NMR (2,4-dinitrotoluene as the internal standard). [d]Reaction run at 150°C. [e]Reaction run at 80°C. [f]6% of **2** was used.

The reaction was also performed in refluxing benzene by using a catalytic ratio **2**/azide/hydrocarbon = 1:15:1000 but compound **3h** was formed in 5 hours with a 60% yield. It is important to point out that the reaction catalysed by **2** is faster than that performed in the presence of Ru(TPP)CO (**1**) where, by using the catalytic ratio **2**/azide/hydrocarbon = 1:15:1000 in refluxing benzene, 77% yield was obtained after 10 hours. This last result indicated that the presence of two pyridine axial ligands did not hamper the efficiency of the catalyst which frees one of the two coordinative sites to activate the azide and promote the hydrocarbon amination.

The reaction time was halved by increasing the methyl hydrocinnamate concentration and, by employing a catalytic ratio **2**/azide/hydrocarbon = 1:15:2500, 70% yield of **3h** was registered in 2.5 hours. Data reported above indicate the importance of using high methyl hydrocinnamate concentrations to achieve good catalytic performances and in turn, to reduce

reaction costs the hydrocarbon excess was recovered at the end of the reaction by a simple distillation process as already reported by us for the same reaction catalysed by complex **1**.[32]

As already stated, the good catalytic activity of complex **2** revealed that the two pyridine ligands are not irreversibly bonded to the metal centre and that a substitution reaction is effective in replacing one of the two pyridine ligands with the azide molecule to trigger the catalytic cycle. To better investigate the strength of the ligation of pyridine to the ruthenium centre of complex **2**, we studied the ligand displacement reaction of pyridine by dimethyl sulfoxide (DMSO). The treating of complex **2** with DMSO yielded $Ru(TPP)(DMSO)_2$ (**4**) in a quantitative yield to support the hypothesis that both the pyridine ligands are weakly coordinated to the metal centre and can be displaced by another electron-donor ligand (Scheme 1).

Taking into account this result, we reacted **2** with an equimolar amount of ArN_3 in order to substitute pyridine with an azide ligand yielding either $Ru^{II}(TPP)(ArN_3)(py)$ (**5**) or $Ru^{IV}(TPP)(ArN)(py)$ (**6**), which derives from complex **5** after the molecular nitrogen departure (Scheme 1). Unfortunately, we did not observe the coordination of one molecule of ArN_3 ligand to the metal centre forming **5** or the formation of the *mono*-imido derivative **6**. The NMR analysis of the reaction crude revealed the presence of an equimolar mixture of $Ru(TPP)(py)_2$ (**2**) and *bis*-imido complex $(Ru(TPP)(NAr)_2$ (**7**) to suggest that, even if compounds **5** and **6** must be momentarily formed, they are too elusive to be experimentally detected and are quickly transformed into **7**. It is reasonable to propose that the presence of the two weakly bonded pyridine ligands can further favour the formation of the thermodynamically stable complex **7.**

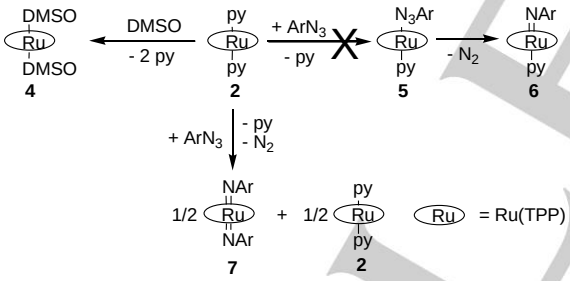

Scheme 1. The reactivity of complex **2** towards DMSO or ArN_3.

Then, we tried to detect the formation of the key intermediate $Ru^{IV}(TPP)(ArN)(py)$ (**6**) by reacting equimolar amounts of $Ru^{II}(TPP)(py)_2$ (**2**) and $Ru^{VI}(TPP)(NAr)_2$ (**7**). Unfortunately, the desired nitrene transfer reaction from **7** to **2** did not occur and the formation of the elusive *mono*-imido intermediate **6** was not observed (Scheme 2).[20,27]

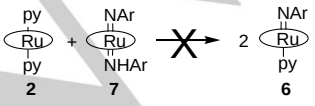

Scheme 2. Reaction between complexes **2** and **7**

In conclusion, all the collected experimental data indicate that the catalytic activity of the *bis*-pyridine complex $Ru(TPP)(py)_2$ (**2**) in the amination of C-H bonds by aromatic azides is comparable to that of Ru(TPP)CO (**1**). This indicates that the electronic characteristic of the axial ligand on the ruthenium centre (CO or pyridine) does not determine the catalytic activity of the corresponding ruthenium catalyst and similar mechanisms for the nitrene transfer reaction can be envisaged.

In order to elucidate this statement, similarities and differences between catalytic aminations promoted by **1** or **2** were studied from a theoretical point of view. The molecular and electronic underpinning of the **2**-promoted reaction mechanism can be tackled with some confidence in view of our previous computational studies of the amination of allylic C-H bonds catalysed by Ru(TPP)CO (**1**).

Computational studies

In a previous computational study, we suggested that the mechanism of the allylic amination of cyclohexene[27] by an organic azide (RN_3) catalysed by [Ru](CO) (**1'**) ([Ru] = Ru(porphine))[44] consists in the two interconnected cycles (**a**) and (**b**) reported in Scheme 3. This proposal was supported by kinetic investigations and by the isolation and characterisation of the key *bis*-imido intermediate $\mathbf{E_S}$ in which R is an aromatic group.[18, 20]

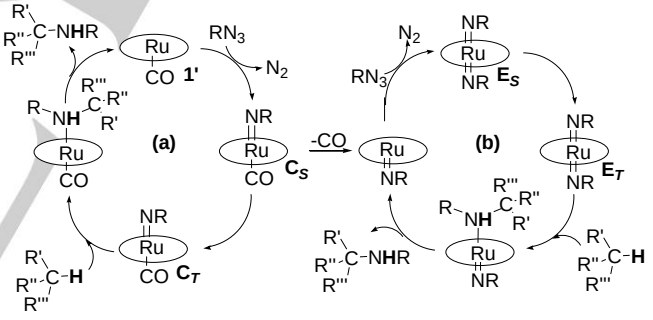

Scheme 3. Proposed mechanisms of the **1'**-catalised C−H amination of cyclohexene (R'R''R'''CH) by RN_3.

The left-side cycle (**a**) corresponds to the first azide activation over the catalyst **1'**.[45] By using methyl azide ($RN_3 = CH_3N_3$) as a model,[46] a barrier of +26.8 kcal mol^{-1} is encountered over the singlet Potential Energy Surface (PES) (but the height is about 25% lower by modelling RN_3 as the experimentally used 3,5-*bis*-trifluoromethyl phenyl azide). Then, the attained *mono*-imido complex [Ru](CO)(NR) ($\mathbf{C_S}$) (R = CH_3) has two alternative evolutions. The first pathway starts with the formation of the triplet isomer [Ru](CO)(NCH_3) ($\mathbf{C_T}$), which is more stable than $\mathbf{C_S}$ by -3.7 kcal mol^{-1} and can allow a radical reactivity. In fact, the two unpaired electrons, being more significantly localised at the axial imido N atom rather than at the metal centre, can promote the activation of one C-H bond of an organic substrate (*e.g.,* cyclohexene for the allylic amination catalysed by **1'**). The *mono*-amido [Ru](CO)($NHCH_3$) complex is formed, together with

the cyclohexyl radical species R'R''R'''C•, by the homolytic cleavage of the cyclohexene C-H bond and then a *'rebound mechanism'*[43] is responsible for the formation of the desired allylic amine. The estimated free energy gain for this process is -44.8 kcal mol^{-1}.[27] Cycle (**b)** in scheme 3 was previously shown to support allylic amination catalysis based on the active biradical species [Ru](NR)$_2$ (**E$_T$**). In the following theoretical analysis will be shown that the species in question is also attainable starting from the *bis*-pyridinate complex **2**, hence the same mechanism also applies in the case of benzylic amination.

Catalytic activity of [Ru](CO) (1') vs. [Ru](py)$_2$ (2')

Since it had been experimentally established the general viability of Ru(TPP)CO-catalysed aminations of both allylic and benzylic substrates,[19, 20] the two reactions were compared also from the computational point of view. Indeed, the replacement of an allylic substrate[27] with a benzylic one did not afford great differences. The energetic profile in Scheme 4 indicated that the activation of a benzylic C-H bond mirrors the C-H allylic activation over **C$_T$** (cycle (**a**) of Scheme 3), which was already illustrated in ref. 27. Thus, the energy barrier at the Transition State {[Ru](CO)(NCH$_3$)$_T$*PhCH$_3$}$_{TS}$ (**8'$_{TS}$**) (Figure S1, R'R''R'''CH = toluene) was only slightly higher than the corresponding one with cyclohexene as the organic substrate (+9.1 *vs*. +7.5 kcal mol^{-1}). Similarly to the allylic amination, the amido complex [Ru](CO)(NHCH$_3$)$_D$ (**9'$_D$**) is first attained from **8'$_{TS}$** and implies the separation of two radicals, which recombine into the final diamagnetic amino complex [Ru](CO)(HN(CH$_3$)CH$_2$Ph) (**10'**). The amine ligand separation from the latter species is energetically more expensive than that of the corresponding allylic amine (+19.2 *vs*. +12.9 kcal mol^{-1}). Such a difference also reflects in the overall energy balance of the amination which is somewhat less exergonic for toluene *vs*. cyclohexene (-37.2 *vs*. -44.8 kcal mol^{-1}. respectively).

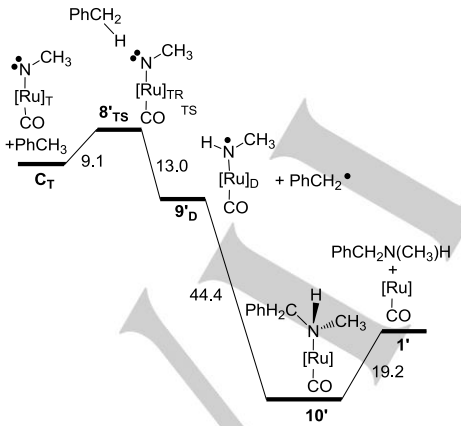

Scheme 4. Energy profile for the benzylic amine formation from the *mono*-imido [Ru](NCH$_3$) (**C$_T$**) species.

The data described up to now showed rather similar mechanistic behaviours for allylic and benzylic aminations catalysed by [Ru](CO) (**1'**). By considering the good catalytic activity of complex Ru(TPP)(py)$_2$ (**2**) described in the experimental section, our interest turned on the catalytic effect of the ruthenium axial ligand. The following DFT analysis was focused on the influence of pyridine axial ligand(s) in the benzylic amination of PhCH$_3$ by CH$_3$N$_3$ starting from [Ru](py)$_2$ (**2'**). The latter species was optimised as the stable species presented in Figure S2. Remarkably, the main geometric parameters fully match with those of an available X-ray structure[47,48] and, in particular, the experimental and computed Ru-N$_{pyridine}$ distances are identical (2.09 Å). In order to behave as a catalyst, **2'** must first dismiss one pyridine ligand as corroborated by the optimisation of the five-coordinated complex [Ru](py) (**11'**) (Figure 1a) although at the not small energy cost of +22.1 kcal mol^{-1} (first step of Scheme 5). Even if the attainment of the unsaturated complex is not straightforward, it must be recalled that the significant experimental temperature (70° C) may help to overcome such a disfavoured step. Then, the process continues with the anchoring of an azide molecule, forming [Ru](py)(CH$_3$N$_3$) (**5'**) (Figure 1b), and the N$_2$ release, which is already in progress at the transition state [Ru](py)(CH$_3$N$_3$)$_{TS}$ (**5'$_{TS}$**) in Figure 2.

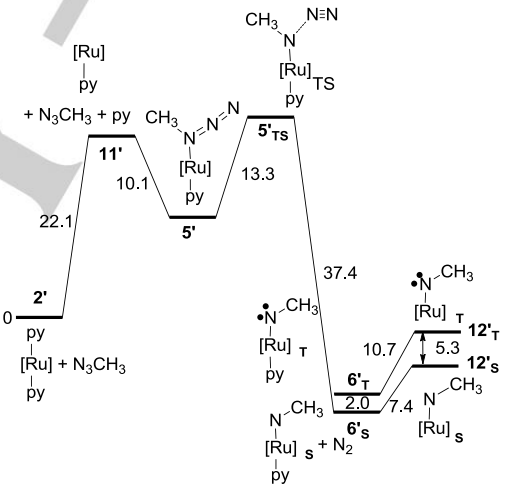

Scheme 5. Energy profile for the formation of *mono*-imido [Ru](NCH$_3$) (**12'**) species.

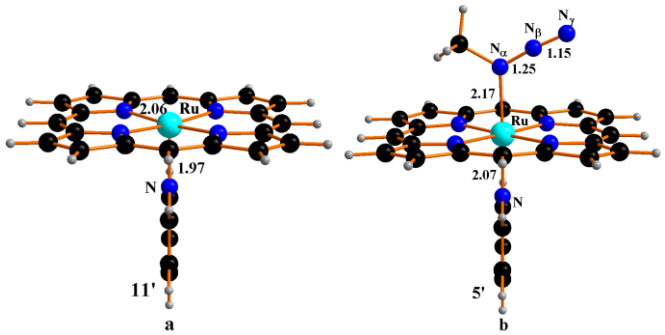

Figure 1. Optimised structure of a) [Ru](py) (**11'**) and b) [Ru](py)(CH$_3$N$_3$) (**5'**).

Energetically, the adduct **5'** appears to be more easily formed than its carbonyl analogue [Ru](CO)(CH_3N_3) (-10.1 vs. -3.5 kcal mol^{-1}) and this step allows to recover about half of the energy already spent for the pyridine ligand dismissal. This point is also consistent with a definitely shorter Ru-N_{azide} distance in **5'** *vs.* [Ru](CO)(CH_3N_3) (2.17 Å *vs.* 2.31 Å). From another viewpoint, the stronger σ *trans* influence exerted by the CO ligand determines the major weakening of the opposite Ru-N bond, which, as shown by specific DFTD calculations,[49] is largely supported only by dispersion interactions, extending to the entire porphyrin ring.[27]

As in other transition states of the azide activation process, also in **5'$_{TS}$** (Figure 2) N_2 is about to be released, being the N_β-N_γ distance as short as 1.14 Å and the N_α-N_β one already large (1.58 Å). Moreover, the N_3 grouping is far from linearity, the angle N_α-N_β-N_γ being 137.2°. Scheme 5 shows that the energy barrier at **5'$_{TS}$** (+13.3 kcal mol^{-1}) is about half with respect to the formation of the corresponding [Ru](CO)(CH_3N_3)$_{TS}$ species (+26.8 kcal mol^{-1}). The result is in line with the metastable character of the complex **5'**, which just for this reason may be particularly efficient as a catalyst.

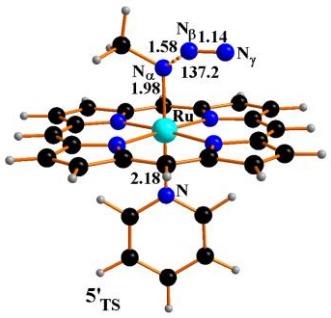

Figure 2. Optimised structure of [Ru](py)(CH_3N_3)$_{TS}$ (**5'$_{TS}$**).

The transformation of **5'$_{TS}$** into the imido complex [Ru](py)(NCH_3)$_S$ (**6'$_S$** in Figure 3a) is largely exergonic (-37.4 kcal mol^{-1}).

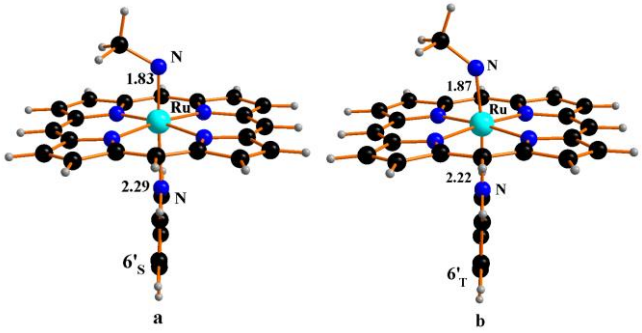

Figure 3. Optimised structure of the spin isomers: a) [Ru](py)(NCH_3)$_S$ (**6'$_S$**) and b) [Ru](py)(NCH_3)$_T$ (**6'$_T$**).

This product compares with the singlet **C$_S$** obtained from **1'**, although its subsequent conversion into the reactive triplet **6'$_T$** (Figure 3b) is slightly disfavoured (+2.0 kcal mol^{-1}) with respect to the analogous formation of **C$_T$** (-3.7 kcal mol^{-1}). In any case, this difference does not exclude the subsequent radical reactivity toward an organic substrate promoted by **6'$_T$**. The intersystem crossing is fundamental for this type of reactivity and it has been proposed also in the case of the *bis*-imido species **E$_S$** and **E$_T$** (+16.1 kcal mol^{-1}), which are operative in the catalytic cycle (**b**) at the right side of Scheme 3 (see below). In that case, the free energy cost was remarkably larger than the +2.0 kcal mol^{-1} value, which was found for the **6'$_S$/6'$_T$** interconversion.

In the absence of the π-acceptor capabilities of CO, the pyridine ligand also determines some different distribution of the unpaired electrons at the imido group of [Ru](py)(NCH_3)$_T$ (**6'$_T$**) *vs.* that of [Ru](CO)(NCH_3)$_T$ (**C$_T$**). This clearly emerges from the comparison of the two singly occupied levels (SOMOs) of the two species. In general, these correspond to combinations of the two metal d_π orbitals (d_{xz}, d_{yz}) with the corresponding N imido p_π orbital of which one is bent.[27] However, in **6'$_T$** the overall spin density at the N atom (Figure S3) is significantly smaller than in **C$_T$** (0.9 *vs*. 1.59 $e^2/bohr^3$), while the associated Ru atom is richer in spin (0.72 *vs*. 0.31 $e^2/bohr^3$). Therefore, not only the energies but also the spin density distributions are key factors in supporting the radical reactivity and the '*rebound mechanism*'. Thus, while the triplet **6'$_T$** is energetically easy to access from the active catalytic species, its radical reactivity appears more hindered due to the reduced spin density at the N atom. Importantly, both **C$_T$** and **6'$_T$** in their radical chemistry follow a rather similar activation mechanism as corroborated by profiles in Schemes 4 and 6.

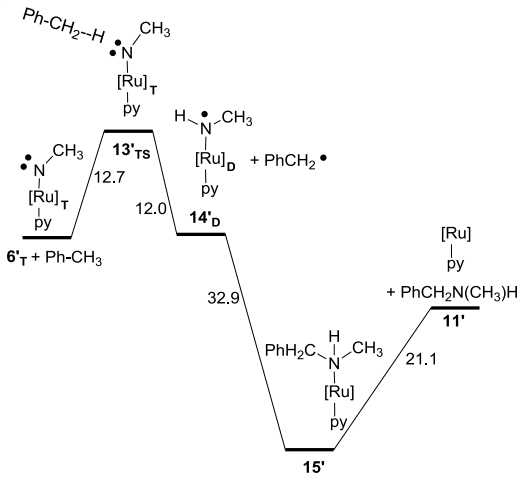

Scheme 6. Energy profile for the benzylic amine formation.

In the Scheme 6, the first optimised adduct is the transition state **13'$_{TS}$** (Figure 4), with a well established interaction between the benzylic methyl and imido groups. At this point, one H atom is almost equally shared by the C and N ones, given that the C···H and H···N separations are 1.34 and 1.28 Å, respectively. The free

energy barrier associated to the formation of **13'$_{TS}$** is somewhat higher than that to reach the transition state {[Ru](CO)(NCH$_3$)$_T$*PhCH$_3$}$_{TS}$, which arises from the combination of **C$_T$** with PhCH$_3$ (+12.7 *vs*. +9.1 kcal mol^{-1} during the toluene amination initiated by **2'** (or better **11'**) and **1'** respectively).

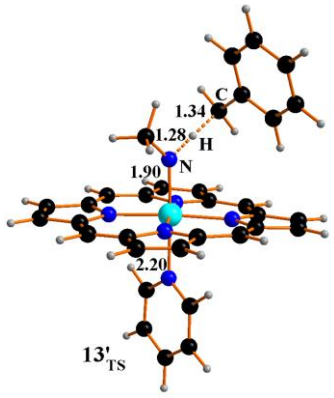

Figure 4. Optimised structure of ([Ru](py)(NCH$_3$)$_T$*(PhCH$_3$)$_{TS}$ (**13'$_{TS}$**).

Interestingly, the analogous barrier for the cyclohexene addition to **C$_T$** is almost identical (+9.0 kcal mol^{-1})[27] to that of toluene, corroborating the general viability of radical mechanisms of these reactions. At **13'$_{TS}$**, a significant spin density is already transferred to the exocyclic carbon atom of toluene and the spin values for Ru, N(imido) and C(toluene) atoms are 0.36, 0.98 and 0.60 e^2/bohr^3, respectively. Upon the complete release of the radical PhCH$_2$•, the doublet [Ru](py)(NHCH$_3$)$_D$ (**14'$_D$** in Figure 5a) is formed with a free energy gain of -12.0 kcal mol^{-1}. Now, the largest radical character is at the N atom of the amidic NHCH$_3$ group, since the corresponding N spin density is 0.61 e^2/bohr^3, which is almost twice as large as the Ru atom spin value (0.3 e^2/bohr^3).

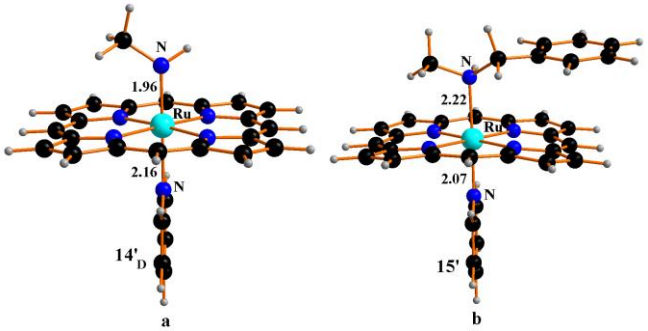

Figure 5. Optimised structure of: a) ([Ru](py)(NHCH$_3$)$_D$ (**14'$_D$**) and b) [Ru](py)(HN(CH$_3$)CH$_2$Ph) (**15'**).

A new N-C coupling becomes possible between the amido and tolyl radicals, given that PhCH$_2$• has an almost equivalent spin concentration at the exocyclic carbon atom (0.61 e^2/bohr^3). The formation of the PhCH$_2$N(CH$_3$)H ligand completes the rebound mechanism yielding the diamagnetic complex [Ru](py)(HN(CH$_3$)CH$_2$Ph)$_S$ (**15'** in Figure 5b) with the large exergonic balance of -32.9 kcal mol^{-1}. Conversely, the separation of the benzylic amine PhCH$_2$N(CH$_3$)H from **15'** is endergonic (+21.1 kcal mol^{-1}) and comparable to the initial loss of one pyridine ligand from [Ru](py)$_2$ (**2'**) to give the five coordinated species **11'** as the active catalyst. Overall, the free energy balance for the benzylic amination (Eq. 1) is more exergonic by using the pyridine complex **11'** in place of the carbonilated **1'** (−43.3 *vs*. −37.2 kcal mol^{-1}, respectively).

$$CH_3N_3 + PhCH_3 \rightarrow PhCH_2N(CH_3)H + N_2 \qquad \text{Eq. 1}$$

Once again, it is worth underlining that, while [Ru](CO) (**1'**) is directly available for the azide activation, the pentacoordinated species [Ru](py) (**11'**) must be obtained from the *bis*-pyridinate precursor [Ru](py)$_2$ (**2'**) with the significant energy cost of +22.1 kcal mol^{-1}. Perhaps this is an indication of a slower starting of the process, which is difficult to be experimentally corroborated in view of the high temperatures needed to run the catalysis

Benzylic amination catalysed by [Ru](NR)$_2$

For the allylic amination promoted by the catalyst [Ru](CO) (**1'**), it was pointed out that the *mono*-imido singlet [Ru](CO)(NCH$_3$) (**C$_S$**) may not invariably convert into the triplet **C$_T$**, but the species may evolve with the CO ligand departure to form the five coordinated complex [Ru](NCH$_3$). In this manner, the right side cycle (**b**) of Scheme 3 can be accessed. Although no *mono*-imido species of the type **C$_S$** or **C$_T$** was ever been experimentally characterised, its computational probe well accounts for a series of experimental facts. Thus, the unsaturated species [Ru](NCH$_3$) can activate a second azide molecule, as complex **1'** does, and generate the *bis*-imido singlet [Ru](NCH$_3$)$_2$ (**E$_S$**). This can also convert into a triplet isomer (**E$_T$**) although with the significant energy cost of +16.1 kcal mol^{-1} which is not a problem in view of the high working temperature of 70° C. The so-formed *bis*-imido species can be involved into an intersystem crossing and then a radical activation of a C-H bond (allylic or benzylic) may be triggered associated to a subsequent '*rebound mechanism*'. As already reported,[27] the allylic amine formation was found to have the still significant the exergonic balance of -40.6 kcal mol^{-1}. Present computational studies indicate that also the process starting with [Ru](py)$_2$ (**2'**) converge at some point into the *bis*-imido diamagnetic complex [Ru](NCH$_3$)$_2$ (**E$_S$**) which, upon the intersystem crossing to the triplet isomer **E$_T$**, also supports the radical activation of toluene. To have a better quantitative evaluation also of the benzylic amination, specific calculations were carried out on the amination of PhCH$_3$ catalysed by [Ru](NCH$_3$)$_2$ (**E$_T$**).

It was found that the initial adduct [**E$_T$***PhCH$_3$]$_{TS}$ (**16'$_{TS}$**) (Figure 6) is also a key transition state with a ΔG barrier of +10.4 kcal mol-1, which is somewhat smaller than that estimated for the amination of cyclohexene (+14.0 kcal mol^{-1}).[50] After the formation of **16'$_{TS}$**, other evident energy differences emerge: i) the separation of the organic radical from the amido-imido doublet [Ru](NHCH$_3$)(NCH$_3$)$_D$ is exergonic by -16.4 and -26.8

kcal mol^{-1} for the toluene and cyclohexene amination, respectively; ii) the '*rebound mechanism*' to form the tolyl amine complex [Ru](NCH$_3$)(HN(CH$_3$)CH$_2$Ph) (**17'**) (Figure 7) is more exergonic (*i.e.,* -36.0 *vs*. -27.8 kcal mol^{-1} for the toluene and cyclohexene amination respectively), iii) the energy cost to release the amine product is about halved (+10.5 *vs*. +21.1 kcal mol^{-1} for benzylic and allylic amine respectively).

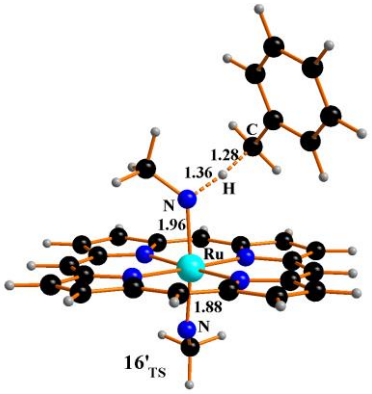

Figure 6. Optimised structure of [$\mathbf{E_T}$*PhCH$_3$]$_{TS}$ (**16'$_{TS}$**).

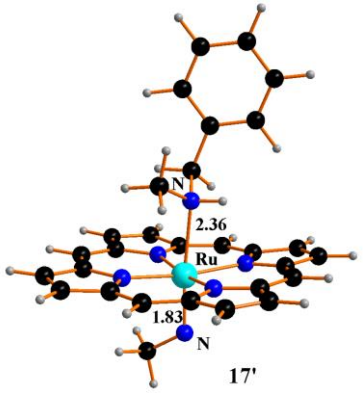

Figure 7. Optimised structure of [Ru](NCH$_3$)(NH(CH$_3$)CH$_2$Ph) (**17'**).

It may be concluded that both the catalytic processes promoted by **1'** or **2'** (or more specifically **11'** in the latter case) consist of two interconnected cycles as pictured in Scheme 3, concerning the toluene substrate, the cycle (**a**) is more favoured over **11'** rather than over the carbonilated **1'** (-43.2 *vs*. -37.2 kcal mol^{-1}). The computational results suggest an identical catalytic activity for the **11'** and the *bis*-imido $\mathbf{E_T}$ (-43.2 *vs*. -43.3 kcal mol^{-1}).

Conclusions

The present work illustrates the experimental catalytic activity of Ru(TPP)(py)$_2$ (**2**) to promote the C-H bond aminations by using electron withdrawing aryl azides. Complex **2** appears as active as Ru(TPP)(CO) (**1**) suggesting a low dependence of the catalytic activity on the electronic characteristic of the axial ligands at the ruthenium centre. Experimental data indicate that one of the two pyridine ligands must be lost to allow the subsequent azide's activation at the vacated coordination site. To investigate the role of the axial ligand on the catalytic efficiency, DFT calculations have monitored the system's evolution starting from the pre-catalyst [Ru](py)$_2$ (**2'**) which forms the active [Ru](py) **(11')** after losing one pyridine ligand. This complex affords azide's activation with the known eco-friendly N_2 release. Importantly, the formation of **11'** from **2'** has the non small energy cost of +22.1 kcal mol^{-1} but, as mentioned, the process seems feasible in view of the high experimental reaction temperature. Because **11'** is a metastable species, the azide activation encounters an about 25% lower barrier with respect to the process initiated by **1'**. Both the *mono*-imido singlet complexes [Ru](py)(NCH$_3$) (**6'$_S$**) and [Ru](CO)(NCH$_3$) (**C$_S$**)[27] can similarly undergo an intersystem crossing that generates either **6'$_T$** or **C$_T$**. These species promote the radical activation of the organic substrate, then completed by the '*rebound mechanism*'. Although the triplet **6'$_T$** appears energetically less accessible than the corresponding **C$_T$** one and the apical N atom has less local spin density, the two processes seem to follow an equal mechanism. The two systems become fully equivalent when the *bis*-imido species $\mathbf{E_S}$ and $\mathbf{E_T}$ are attained from different precursors (cycle (**b**) in Scheme 3). Independently from the nature of the axial ligands, it may be concluded that, both the allylic and benzylic aminations involve the two interconnected catalytic cycles reported in Scheme 3 with comparable free energy balances.

Experimental Section

General Conditions. All reactions were performed under a nitrogen atmosphere employing standard Schlenk techniques and vacuum-line manipulations. Benzene, toluene, cyclohexene, cumene, pyridine and dichloromethane were purified by distillation under nitrogen over CaH_2 or Na. All the other starting materials were commercial products used after degasification.

Solvents and reagents. 3,5-*Bis*(trifluoromethyl)phenyl azide,[51] 4-*tert*-butylphenyl azide[52], $TPPH_2$,[53] Ru(TPP)(CO) (**1**),[54] Ru(TPP)(CO)(MeOH),[35] Ru(TPP)(py)$_2$ (**2**),[40] Ru(TPP)(NAr)$_2$ (**7**) (Ar = 3,5-*bis*(trifluoromethyl)phenyl),[18] and methyl hydrocinnamate[55] were synthesised by methods reported in the literature or using minor modification of them.

Instruments. NMR spectra were recorded at 300 K (unless otherwise specified) operating either at 300 MHz or at 400 MHz for 1H. Infrared spectra, UV/vis spectra, and mass spectra were recorded in the analytical laboratories of Milan University.

Computational details. All the calculations were carried out with the Gaussian 09 package[56] at B97D-DFT[49] level of theory. All the optimised structures were validated as minima and/or transition states by computed vibrational frequencies. All the calculations were based on the CPCM [57] model for the benzene solvent, the same used in the experiments. The effective Stuttgart/Dresden core potential (SDD)[58] was adopted for the ruthenium center, while for all the other atomic species the basis set was 6-31G, with the addition of the polarisation functions (d,p). The

coordinates of all the optimised structures are reported in the Supporting Information.

Synthesis of Ru(TPP)(DMSO)$_2$ (4).[59] Ru(TPP)(py)$_2$ (13.7 mg, 1.54×10^{-2} mmol) was suspended in 2.0 mL of DMSO and the resulting solution was heated at 110°C for 4.0 h. The solution was evaporated to dryness and the crystalline violet solid was dried *in vacuo*. Analytical data are in accord with those reported in the literature.

General procedures for catalytic reactions. In a typical run, the aryl azide and the ruthenium catalyst (6.0 mg, 6.8×10^{-3} mmol) were dissolved into the hydrocarbon (15 mL). The resulting mixture was heated using a preheated oil bath until the complete consumption of the azide. The catalytic reaction was monitored by IR spectroscopy by measuring the characteristic N_3 absorbance at ~2115 cm^{-1}. The reaction was considered finished when the absorbance value of the azide was below 0.01 (by using a 0.1 mm thick cell). The solvent was evaporated to dryness and the residue analysed by ^{1}H-NMR analysis using 2,4-dinitrotoluene as the internal standard.
Analytical data of **3a**[19], **3b**[19], **3c**[60], **3d**[19], **3e**[19], **3f**[19], **3g**[32], **3h**[32], **3i**[61] are in accord with those reported in literature.

Acknowledgements

C. M. and G. M. acknowledge the ISCRA-CINECA HP grant 'HP10BEG2NO' and CREA (Centro Ricerche Energia e Ambiente) of Colle Val d'Elsa (Siena, Italy) for computational resources.
Keywords: Ruthenium • Porphyrin • C-H amination • Theoretical study

[1] E. Dux, *Chem. Rev.* **2009**, *19*, 11-15.
[2] J. C. Lewis, R. G. Bergman, J. A. Ellman, *Acc. Chem. Res.* **2008**, *41*, 1013-1025.
[3] *Organic Azides Syntheses And Applications* (Eds.: S. Bräse, K. Banert) John Wiley & Sons Ltd., 2010.
[4] S. Bräese, C. Gil, K. Knepper, V. Zimmermann, *Angew. Chem. Int. Ed.* **2005**, *44*, 5188-5240.
[5] S. Cenini, E. Gallo, A. Caselli, F. Ragaini, S. Fantauzzi, C. Piangiolino, *Coord. Chem. Rev.* **2006**, *250*, 1234-1253.
[6] S. Cenini, F. Ragaini, E. Gallo, A. Caselli, *Curr. Org. Chem.* **2011**, *15*, 1578-1592.
[7] S. Chiba, *Synlett* **2012**, 21-44.
[8] T. G. Driver, *Org. Biomol. Chem*. **2010**, *8*, 3831-3846.
[9] T. Katsuki, *Chem. Lett.* **2005**, *34*, 1304-1309.
[10] M. Minozzi, D. Nanni, P. Spagnolo, *Chem. Eur. J*. **2009**, *15*, 7830-7840.
[11] M. Y. Weber, G.; Wille, G., *Chimica Oggi* **2011**, *29*, 8-10.
[12] S. Cenini, E. Gallo, A. Penoni, F. Ragaini, S. Tollari, *Chem. Commun*. **2000**, 2265-2266.
[13] S. Fantauzzi, A. Caselli, E. Gallo, *Dalton Trans*. **2009**, 5434-5443.
[14] F. Ragaini, A. Penoni, E. Gallo, S. Tollari, C. L. Gotti, M. Lapadula, E. Mangioni, S. Cenini, *Chem. Eur. J*. **2003**, *9*, 249-259.
[15] A. Caselli, E. Gallo, S. Fantauzzi, S. Morlacchi, F. Ragaini, S. Cenini, *Eur. J. Inorg. Chem.* **2008**, 3009-3019.
[16] T. W.-S. Chow, G.-Q. Chen, Y. Liu, C.-Y. Zhou, C.-M. Che, *Pure Appl. Chem*. **2012**, *84*, 1685-1704.
[17] S. Fantauzzi, E. Gallo, A. Caselli, C. Piangiolino, F. Ragaini, S. Cenini, *Eur. J. Org. Chem*. **2007**, 6053-6059.
[18] S. Fantauzzi, E. Gallo, A. Caselli, F. Ragaini, N. Casati, P. Macchi, S. Cenini, *Chem. Commun*. **2009**, 3952-3954.
[19] D. Intrieri, A. Caselli, F. Ragaini, S. Cenini, E. Gallo, *J. Porphyrins Phthalocyanines* **2010**, *14*, 732-740.
[20] D. Intrieri, A. Caselli, F. Ragaini, P. Macchi, N. Casati, E. Gallo, *Eur. J. Inorg. Chem.* **2012**, 569-580.
[21] D. Intrieri, M. Mariani, A. Caselli, F. Ragaini, E. Gallo, *Chem. Eur. J.* **2012**, *18*, 10487-10490.
[22] Y. Liu, C.-M. Che, *Chem. Eur. J.* **2010**, *16*, 10494-10501.
[23] H.-J. Lu, V. Subbarayan, J.-R. Tao, X. P. Zhang, *Organometallics* **2010**, *29*, 389-393.
[24] H. Lu, H. Jiang, L. Wojtas, X. P. Zhang, *Angew. Chem. Int. Ed*. **2010**, *49*, 10192-10196.
[25] H. Lu, J. Tao, J. E. Jones, L. Wojtas, X. P. Zhang, *Org. Lett.* **2010**, *12*, 1248-1251.
[26] H. Lu, X. P. Zhang, *Chem. Soc. Rev.* **2011**, *40*, 1899-1909.
[27] G. Manca, E. Gallo, D. Intrieri, C. Mealli, *ACS Catal.* **2014**, *4*, 823-832.
[28] C. Piangiolino, E. Gallo, A. Caselli, S. Fantauzzi, F. Ragaini, S. Cenini, *Eur. J. Org. Chem*. **2007**, 743-750.
[29] P. Zardi, D. Intrieri, A. Caselli, E. Gallo, *J. Organomet. Chem.* **2012**, *716*, 269-274.
[30] A. Caselli, E. Gallo, F. Ragaini, F. Ricatto, G. Abbiati, S. Cenini, *Inorg. Chim. Acta* **2006**, *359*, 2924-2932.
[31] H. Lu, Y. Hu, H. Jiang, L. Wojtas, X. P. Zhang, *Org. Lett.* **2012**, *14*, 5158-5161.
[32] P. Zardi, A. Caselli, P. Macchi, F. Ferretti, E. Gallo, *Organometallics* **2014**, *33*, 2210-2218.
[33] C.-M. Che, V. K.-Y. Lo, C.-Y. Zhou, J.-S. Huang, *Chem. Soc. Rev.* **2011**, *40*, 1950-1975.
[34] G. M. Brown, F. R. Hopf, J. A. Ferguson, T. J. Meyer, D. G. Whitten, *J. Am. Chem. Soc.* **1973**, *95*, 5939-5942.
[35] J. P. Collman, C. E. Barnes, P. N. Swepston, J. A. Ibers, *J. Am. Chem. Soc.* **1984**, *106*, 3500-3510.
[36] J. P. Collman, S. T. Harford, S. Franzen, J.-C. Marchon, P. Maldivi, A. P. Shreve, W. H. Woodruff, *Inorg. Chem.* **1999**, *38*, 2085-2092.
[37] S. C. Jeoung, D. Kim, D. W. Cho, M. Yoon, K.-H. Ahn, *J. Phys. Chem.* **1996**, *100*, 8867-8874.
[38] D. Kim, Y. O. Su, T. G. Spiro, *Inorg. Chem.* **1986**, *25*, 3993-3997.
[39] I. R. Paeng, K. Nakamoto, *J. Am. Chem. Soc.* **1990**, *112*, 3289-3297.
[40] S. E. Vitols, R. Kumble, M. E. Blackwood, J. S. Roman, T. G. Spiro, *J. Phys. Chem.* **1996**, *100*, 4180-4187.
[41] M. Barley, D. Dolphin, B. R. James, C. Kirmaier, D. Holten, *J. Am. Chem. Soc.* **1984**, *106*, 3937-3943.
[42] C. D. Tait, D. Holten, M. Barley, D. Dolphin, B. R. James, *J. Am. Chem. Soc.* **1985**, *107*, 1930-1934.
[43] J. T. Groves, *J. Chem. Educ.* **1985**, *26,* 928−931.
[44] For the sake of simplicity, the DFT study was carried out with a porphine ligand having H atoms in place of the phenyl groups in the *meso*-positions of tetraphenyl porphyrin. Analogously, CH_3N_3 was modelled in place of the experimentally used 3,5-*bis*(trifluoromethyl)phenyl azide reactant (ArN_3). In fact, the simplified modelling does not alter the basic functionality of the reactants and the computed mechanism is generally applicable. On the other hand, models closer to the experimental ones cause some lowering of the key barrier but not the reaction profile.
[45] In general, the numbers of the models are primed to underline some possible difference with respect to the experimentally used species.
[46] Even if in the experimental study the R substituent of RN_3 is an aryl group, for computational reasons the DFT investigation was carried out with R = CH_3 and the peripheral *meso*-aryl substituents on the porphyrin ring have been replaced by H atoms.
[47] a) J. P. Collman, J. I. Brauman, J. P. Fitzgerald, J. W. Sparapany, J. A. Ibers, *J. Am. Chem. Soc.* **1988**, *110*, 3486-3495. b) Y. Li, P. W. Hong Chan, N.-Y. Zhu, C.-M. Che, H.-L. Kwong, *Organometallics*, **2004**, *23*, 54-66.
[48] a) F. R. Hopf, T. P. O'Brien, W. R. Scheidt, D. G. Whitten, *J. Am. Chem. Soc.* **1975**, *97*, 277-281. b) F. Malvolti, P. Le Maux, L. Toupet, M. E.

Smith, W. Y. Man, P. J. Low, E. Galardon, G. Simmonneaux, F. Paul, *Inorg. Chem*. **2010**, *49*, 9101-9103.

[49] S. Grimme, *J. Chem. Phys*. **2006**, 3952-3954.

[50] A very reliable comparison between the barriers is not possible, since for technical reasons, the energy of cyclohexene TS was estimated only as ΔE (electronic energy). In these terms, the barrier is higher for cyclohexene than toluene (+3.0 *vs*. +0.2 kcal mol^{-1}), but the difference should remain also in terms of the free energy ΔG, by assuming that the entropic component computed for toluene (-TΔS) is estimated to be +10 kcal mol^{-1}.

[51] M. Tanno, S. Sueyoshi, S. Kamiya *Chem. Pharm. Bull*. **1982**, *30*, 3125-3132.

[52] J. B. Gerken, M. L. Rigsby, R. E. Ruther, R. J. Pérez-Rodríguez, I. A. Guzei, R. J. Hamers, S. S. Stahl, *Inorg. Chem.* **2013**, *52*, 2796-2798.

[53] A. D. Adler, F. R. Longo, J. D. Finarelli, J. Goldmacher, J. Assour, L. Korsakoff, *J. Org. Chem.* **1967**, *32*, 476.

[54] J. P. Collman, A. O. Chong, G. B. Jameson, R. T. Oakley, E. Rose, E. R. Schmittou, J. A. Ibers, *J. Am. Chem. Soc.* **1981**, *103*, 516-533.

[55] A. W. Ingersoll, *Organic Syntheses* **1929**,9.

[56] M. J. Frisch, G. W. Trucks, H. B. Schlegel, G. E. Scuseria, M. A. Robb, J. R. Cheeseman, G. Scalmani, V. Barone, B. Mennucci, G. A. Petersson, H. Nakatsuji, M. Caricato, X. Li, H. P. Hratchian, A. F. Izmaylov, J. Bloino, G. Zheng, J. L. Sonnenberg, M. Hada, M. Ehara, K. Toyota, R. Fukuda, J. Hasegawa, M. Ishida, T. Nakajima, Y. Honda, O. Kitao, H. Nakai, T. Vreven, J. A. Montgomery, Jr., J. E. Peralta, F. Ogliaro, M. Bearpark, J. J. Heyd, E. Brothers, K. N. Kudin, V. N. Staroverov, R. Kobayashi, J. Normand, K. Raghavachari, A. Rendell, J. C. Burant, S. S. Iyengar, J. Tomasi, M. Cossi, N. Rega, J. M. Millam, M. Klene, J. E. Knox, J. B. Cross, V. Bakken, C. Adamo, J. Jaramillo, R. Gomperts, R. E. Stratmann, O. Yazyev, A. J. Austin, R. Cammi, C. Pomelli, J. W. Ochterski, R. L. Martin, K. Morokuma, V. G. Zakrzewski, G. A. Voth, P. Salvador, J. J. Dannenberg, S. Dapprich, A. D. Daniels, Ö. Farkas, J. B. Foresman, J. V. Ortiz, J. Cioslowski, and D. J. Fox, Gaussian 09, Revision B.01,Gaussian, Inc., Wallingford CT, 2009.

[57] a) V. Barone, M. Cossi, *J. Phys. Chem. A* **1998**, *102*, 1995-2001. b) M. Cossi, N. Rega, G. Scalmani, V. Barone, *J. Comput. Chem.* **2003**, *24*, 669-681.

[58] M. Dolg, H. Stoll, H. Preuss, R. M. Pitzer, *J. Phys. Chem.* **1993**, *97*, 5852-5859.

[59] E. Gallo, A. Caselli, F. Ragaini, S. Fantauzzi, N. Masciocchi, A. Sironi, S. Cenini, *Inorg. Chem.* **2005**, *44*, 2039-2049.

[60] S. Zhou, S. Fleischer, H. Jiao, K. Junge, M. Beller, *Adv. Synth. Catal.* **2014**, *356*, 3451-3455.

[61] F. Ragaini, S. Cenini, F. Turra, A. Caselli, *Tetrahedron* **2004**, *60*, 4989-4994.

Entry for the Table of Contents

FULL PAPER

The catalytic activity of Ru(TPP)(py)$_2$ (**2**) in the amination of C-H bonds by organic azides (RN_3) was experimentally compared to that of Ru(TPP)(CO) (**1**). A computational analysis corroborates similar radical mechanisms at a triplet imido intermediate in spite of the electronic differences of the apical ligands.

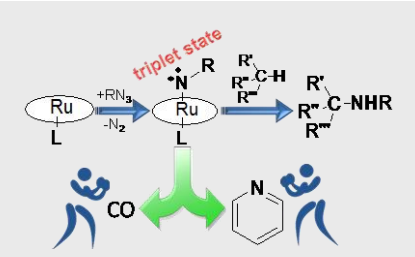

G. Manca, C. Mealli, D. M. Carminati, D. Intrieri and E. Gallo

Page No. – Page No.

Comparative Study of the Catalytic Amination of Benzylic C-H Bonds Promoted by Ru(TPP)(py)$_2$ *vs.* Ru(TPP)(CO).